INFECTION AND IMMUNITY, Oct. 2000, p. 5979–5990 Vol. 68, No. 10
0019-9567/00/$04.00+0

Structural and Functional Lesions in Brush Border of Human Polarized Intestinal Caco-2/TC7 Cells Infected by Members of the Afa/Dr Diffusely Adhering Family of *Escherichia coli*

ISABELLE PEIFFER,[1] JULIE GUIGNOT,[1] ALAIN BARBAT,[2] CHRISTOPHE CARNOY,[3] STEVE L. MOSELEY,[3] BOGDAN J. NOWICKI,[4] ALAIN L. SERVIN,[1]* AND MARIE-FRANÇOISE BERNET-CAMARD[1]

Institut National de la Santé et de la Recherche Médicale (INSERM), Unité 510, Faculté de Pharmacie Paris XI, F-92296 Châtenay-Malabry,[1] and INSERM, Unité 504, F-94407 Villejuif,[2] France; Department of Microbiology, University of Washington, Seattle, Washington 98195-7242[3]; and Division of Infectious Diseases, Department of Obstetrics and Gynecology, and Department of Microbiology, The University of Texas Medical Branch, Galveston, Texas 77550[4]

Received 14 February 2000/Returned for modification 31 May 2000/Accepted 5 July 2000

Diffusely adhering *Escherichia coli* (DAEC) strains expressing F1845 fimbrial adhesin or Dr hemagglutinin belonging to the Afa/Dr family of adhesins infect cultured polarized human intestinal cells through recognition of the brush border-associated decay-accelerating factor (DAF; CD55) as a receptor. The wild-type Afa/Dr DAEC strain C1845 has been shown to induce brush border lesions by an adhesin-dependent mechanism triggering apical F-actin rearrangements. In the present study, we undertook to further characterize cell injuries following the interaction of wild-type Afa/Dr DAEC strains C1845 and IH11128 expressing fimbrial F1845 adhesin and Dr hemagglutinin, respectively, with polarized, fully differentiated Caco-2/TC7 cells. In both cases, bacterium-cell interaction was followed by rearrangement of the major brush border-associated cytoskeletal proteins F-actin, villin, and fimbrin, proteins which play a pivotal role in brush border assembly. In contrast, distribution of G-actin, actin-depolymerizing factor, and tubulin was not modified. Using *draE* mutants, we found that a mutant in which cysteine replaces aspartic acid at position 54 conserved binding capacity but failed to induce F-actin disassembly. Accompanying the cytoskeleton injuries, we found that the distribution of brush border-associated functional proteins sucrase-isomaltase (SI), dipeptidylpeptidase IV (DPPIV), glucose transporter SGLT1, and fructose transporter GLUT5 was dramatically altered. In parallel, SI and DPPIV enzyme activity decreased.

Diffusely adhering *Escherichia coli* (DAEC) strains are considered a heterogeneous group. It has been well established that some Afa/Dr DAEC expressing related adhesins adhere to host cells and cause symptomatic urinary tract and intestinal infections. Afa/Dr DAEC harboring the afimbrial adhesin I (AfaE-I) (34) and adhesin III (AfaE-III) (18, 35), the Dr hemagglutinin (51), and the adhesin DR-II (58) have been associated with 30% of cases of pyelonephritis in pregnant women. Afa/Dr DAEC strain C1845 harboring the fimbrial F1845 adhesin has been isolated from an infant with diarrhea (4). These virulent *E. coli* strains express a family of gene operons, including *afa* (19, 20, 30, 34, 35), *dra* (66), and *daa* (3, 4, 38). Moreover, a common system of adhesion involving the decay-accelerating-factor (DAF; CD55) as a receptor has been identified for Afa/Dr DAEC (48, 50).

Yamamoto et al. (67) were first to report that adherence of DAEC induced elongated cellular projections in epithelial HeLa cells. Cookson and Nataro (10) observed that attachment of Afa/Dr DAEC onto epithelial Hep-2 cells is followed by induction of a long thin membrane extending from the cell surface. Moreover, Afa/Dr DAEC-induced cytoskeletal rearrangements in HeLa cells have been recently reported by Goluszko et al. (23). We have previously shown that Afa/Dr DAEC strains infect polarized human intestinal Caco-2 cells expressing a well-characterized brush border endowed with CD55 and forming a monolayer mimicking an epithelial barrier (32). When investigating the mechanism of pathogenicity of the diarrheagenic Afa/Dr DAEC strain C1845 in Caco-2 cells, we reported that the first event in cell infection is adhesin binding to the apical surface of polarized cells resulting from recognition of the brush border-associated CD55 (2, 33). Bacterial attachment is followed by microvillar injury, characterized by elongation and nucleation of the microvilli (MV) accompanied by cytoskeletal F-actin disassembly (2). Moreover, we have recently demonstrated that Afa/Dr DAEC induced hijacking of CD55-associated signal transduction, promoting cytoskeletal F-actin disassembly through a Ca^{2+}-dependent mechanism in unpolarized embryonic intestinal INT407 cells (54).

We decided to examine in a more detailed fashion how Afa/Dr DAEC strains C1845 and IH11128 promoted damage in polarized cells expressing a brush border and forming a monolayer mimicking an epithelial barrier. Polarity of epithelial cells results in the existence of three domains in the plasma membrane: the apical surface facing the lumen, the lateral surface facing the adjacent cells, and the basal surface underlying the connective tissue. In epithelial intestinal cells, the cytoskeleton is essential for establishment and maintenance of the structural and functional polarized organization of the cells (for reviews, see references 16 and 39). The brush border is composed of a dense lawn of uniform MV, for which the ultrastructure and biochemical composition have been extensively investigated (for a review, see reference 28; also see references 55–57). Distribution of cytoskeletal proteins playing

* Corresponding author. Mailing address: INSERM Unité 510, Faculté de Pharmacie Paris XI, F-92296 Châtenay-Malabry, France. Phone and fax: 33.1.46.83.56.61. E-mail: alain.servin@cep.u-psud.fr.

a pivotal role in brush border assembly was examined. We focused our study on predominant components of microvillar cores, actin, and two actin-binding proteins, villin and fimbrin. In parallel, we examined whether injuries in brush border-associated functional proteins develop in Afa/Dr DAEC-infected cells. We focused our study on four proteins: two hydrolases, the sucrase-isomaltase (SI; EC 3.2.1.10 and EC 3.2.1.48) and dipeptidylpeptidase IV (DPPIV; EC 3.4.14.5), and two carbohydrate transporters, SGLT1 and GLUT5. SI is an α-glucosidase which hydrolyzes maltose, sucrose, and maltotriose. DPPIV is a widely distributed type II membrane glycoprotein which is essential for the intestinal transport of proline-containing peptides. The glucose transporter SGLT1 and the fructose transporter GLUT5 account for the energy-dependent uptake of D-glucose/galactose (concomitant with Na^+ ions) and fructose, respectively.

MATERIALS AND METHODS

Reagents. 4-Amino-antipyrine-1,4-diazabicyclo-(2,2,2) octane (DABCO), glucose oxidase type V, peroxidase type II, Gly-Pro *p*-nitroanilide, L-Ala *p*-nitroanilide, BAPTA/AM (1,2-bis[2-amino-phenoxy]ethane-*N*,*N*,*N*′,*N*′-tetraacetic acid tetrakis [acetoxymethyl] ester), dantrolene (1-[(5-[p-nitrophenyl]furfurylidene)-amino]hydantoin), and all other reagents were obtained from Sigma-Aldrich Chimie SARL (L'Isle d'Abeau Chesnes, France).

Cell line. The Caco-2/TC7 clone (9), established from the cultured human colonic adenocarcinoma parental Caco-2 cell line, which spontaneously differentiates in culture (59), was used. Cells were routinely grown in Dulbecco's modified Eagle's medium (25 mM glucose) (Life Technologies, Cergy, France), supplemented with 15% heat-inactivated (30 min, 56°C) fetal calf serum (Boehringer, Mannheim, Germany) and 1% nonessential amino acids (Life Technologies) as previously described (2). Cells were seeded in 24-well Corning tissue culture plates (Corning Glass Works, Corning, N.Y.) at a concentration of 2.5×10^4 cells per well. For maintenance purposes, cells were passaged weekly using 0.02% trypsin in Ca^{2+}- and Mg^{2+}-free phosphate-buffered saline (PBS) containing 3 mM EDTA. Experiments and maintenance of the cells were carried out at 37°C in a 10% CO_2–90% air atmosphere. The culture medium was changed daily. Cells were used at postconfluence after 15 days of culture (fully differentiated cells) for the infection assay.

Bacterial strains. The clinical isolates *E. coli* C1845, harboring the fimbrial F1845 adhesin (4), and IH11128, harboring the Dr hemagglutinin (51), were grown at 37°C for 18 h on Luria agar.

Mutant strains carrying the pCC90 plasmid in which point mutations in *draE* were created by site-directed mutagenesis were used (8). *E. coli* DH5α(pCC90) carries the plasmid encoding the Dr hemagglutinin. For the mutant strains, threonine-90 is replaced by methionine (pCC90-T90M), isoleucine-113 is replaced by threonine (pCC90-I113T), aspartic acid-54 (Asp-54) is replaced by valine (pCC90-D54V), Asp-54 is replaced by tyrosine (pCC90-D54Y), Asp-54 is replaced by glycine (pCC90-D54G), and Asp-54 is replaced by cysteine (pCC90-D54C).

Cell infection. The method used for DAEC infection of cultured cells has been described previously (2). Briefly, Caco-2/TC7 monolayers were washed twice with PBS. Infecting *E. coli* were suspended in the culture medium, and a total of 0.5 ml (10^8 CFU/well) of this suspension was added to each well of the tissue culture plate. The plates were incubated at 37°C in 10% CO_2–90% air for 3 h. The monolayers were then washed three times with sterile PBS.

Quantification of *E. coli* binding. Quantitative binding assays of *E. coli* onto cultured cells were conducted with metabolically labeled bacteria. *E. coli* was radiolabeled by the addition of [^{14}C]acetic acid (Amersham; 94 mCi/mmol; 100 μCi per 10-ml tube) in Luria broth, as previously reported (2). The cell monolayers were infected with radiolabeled bacteria (10^8 CFU/well, 50,000 to 70,000 cpm) in the presence of 1% mannose to prevent type 1 fimbria-mediated binding and incubated at 37°C in 10% CO_2–90% air for 3 h. The monolayers were then washed three times with sterile PBS. Adhering bacteria and intestinal cells were dissolved in a 1 N NaOH solution. The level of bacterial adhesion was evaluated by liquid scintillation counting. Each adherence assay was conducted in triplicate with three successive cell passages.

Measurement of cell integrity. In each experiment, the integrity of the confluent polarized monolayers was checked by measuring transepithelial membrane resistance (TER) with a volt-ohmmeter (Millicel ERS; Millipore). Moreover, cell integrity in several experiments was determined by measuring lactate dehydrogenase (LDH) in the culture medium posttreatment (Enzyline LDH kit; Biomérieux, Dardilly, France).

Electron microscopy. For transmission electron microscopy, cells were rinsed three times with PBS and fixed with 2.5% glutaraldehyde in 0.1 M sodium phosphate buffer (pH 7.4) for 30 min at room temperature. After being washed with PBS, cells were postfixed for 30 min at room temperature with 1.5% osmium tetroxide in sodium phosphate buffer. Filters were then dehydrated in a graded ethanol series, cut into strips, and embedded in epoxy resin. Ultrathin sections were cut from transversely oriented confluent monolayers. Ultrathin sections were double stained with uranyl acetate and lead citrate and examined with a Jeol JEM-1010 electron microscope.

Antibodies. Fluorescein isothiocyanate (FITC)-phalloidin-labeled F-actin was from Molecular Probes Inc. (Eugene, Oreg.). Monoclonal antibody (MAb) JLA20 against G-actin was from Biovallet (Marne-la-Vallée, France). The polyclonal antibodies directed against fimbrin and villin (serum 1.135) were kindly provided by M. Arpin and S. Robine (Institut Curie, UMR 144, Paris, France). The rabbit polyclonal antibody directed against actin-depolymerizing factor (ADF) was kindly provided by J. Bamburg (Colorado State University, Fort Collins, Colo.). MAbs and polyclonal antibodies directed against α-actinin, tubulin, and cytokeratin 18 were from Sigma (St. Louis, Mo.). The MAbs anti-human DPPIV antibody (4H3) and anti-human SI antibody (8A9) were a gift from S. Maroux (ESA 6033 CNRS, Marseille, France) (diluted 1:50 in 0.2% gelatin–PBS and 1:200 in 0.2% gelatin–PBS, respectively). The MAbs directed against the fructose transporter GLUT5 and glucose transporter SGLT1 were kindly provided by E. Brot-Laroche (INSERM, U505, Paris, France) (diluted 1:500 and 1:50 in 0.2% gelatin–PBS, respectively). The appropriate secondary tetramethyl rhodamine isothiocyanate (TRITC)-conjugated and FITC-conjugated antibodies were obtained from Boehringer and Immunoresearch ICN Laboratory and were diluted 1:20 to 1:200 in 0.2% gelatin–PBS.

Immunofluorescence. Cell monolayers were prepared on glass coverslips, which were placed in 24-well tissue culture plates (Corning Glass Works).

When G-actin, ADF, α-actinin, fimbrin, villin, and cytokeratin 18 were to be visualized, coverslips were permeabilized by incubation with 0.2% Triton X-100 in PBS for 4 min, and the coverslips were then rewashed three times with PBS. Permeabilized cell monolayers were incubated with specific primary antibody (diluted 1:50 to 1:200 in PBS in 0.2% gelatin–PBS) for 45 min at room temperature, washed, and then incubated with their respective secondary TRITC- or FITC-conjugated antibody used at a dilution of 1:20 to 1:200 in 0.2% gelatin–PBS. No fluorescent staining was observed when nonimmune serum was used and when the primary antibody was omitted.

To visualize F-actin, coverslips were permeabilized by incubation with 0.2% Triton X-100 in PBS for 4 min at room temperature before incubation with FITC-phalloidin for 45 min at 22°C. The coverslips were then rewashed three times with PBS.

The brush border-associated proteins were stained by indirect immunofluorescence labeling. Immunolabeling was conducted without cell permeabilization in cells fixed with 3% paraformaldehyde for 15 min at room temperature, washed three times with PBS, and then treated with 50 mM NH_4Cl for 10 min (for aldehyde function saturation). Fixed monolayers were incubated with each specific primary antibody described above for 45 min at room temperature. After three washes in PBS, incubation with a FITC- or TRITC-conjugated second antibody was performed for 45 min at room temperature. No fluorescent staining was observed when nonimmune serum was used and when the primary antibody was omitted.

Specimens were mounted in Vectashield mounting medium (Vector Laboratory, Burlingame, Calif.). Specimens were examined by epifluorescence using a Leitz Aristoplan microscope with epifluorescence. Moreover, a confocal analysis was conducted using a confocal laser scanning microscope (model PCM 2000; air-cooled argon ion laser 457, 488, and 514 nm; Nikon, Badhoevedorp, The Netherlands) configured with a Nikon Diaphot 300 microscope using a 100× Pan Fluor ELSW DM CF160 objective. Optical sectioning was used to collect 50 en face images 0.3 to 0.4 μm apart. Lateral views were obtained by integration of 100 images gathered at a step position of 1 on the *x*-*y* axis using the accompanying Nikon E2-2000 software on Windows NT. Photographic images were resized, organized, and labeled using Adobe Photoshop software (San Jose, Calif.). The printed images (Kodak XLS 8600 PS; Eastman Kodak Co., Rochester, N.Y.) are representative of the original data. All photographs were taken on Kodak electronic imaging paper (Eastman Kodak Co.).

Quantification of rearrangements of brush border-associated proteins. Relative immunofluorescence intensity was measured with a conventional fluorescent microscope (model Aristoplan; Leitz) connected to the Image Analyzer Visiolab 1000 (Biocom, Les Ulis, France). Results are expressed as arbitrary units.

To quantify the number of cells presenting F-actin disassembly, images were acquired from the fluorescent microscope equipped with a charge-coupled device camera (Sony, Tokyo, Japan) connected to the Image Analyzer Visiolab 1000. Typically, the image was focused on the apical side of the cells. One image per field including 30 cells was recorded. More than 10 fields per monolayer were examined, representing examination of 300 to 400 individual cells. F-actin disassembly was scored as previously reported (54) in a blind review of about 20 monolayers resulting from six experiments conducted with successive passages of Caco-2/TC7 cells. The results are presented as the mean ± standard error of the mean (SEM) of the percentage of cells presenting apical F-actin disorganization relative to the total number of cells.

Enzyme assay. Cells were washed in ice-cold PBS, scraped, suspended in H_2O, and homogenized. Enzyme activities were measured in an enriched membrane fraction obtained after 1 h of centrifugation of the cell homogenates at 100,000 × *g* and 4°C. SI and DPPIV enzyme activities were assayed as previously described (29). Enzyme specific activity was expressed as milliunits per milligram of protein. One unit is defined as the amount of enzyme that hydrolyzes 1 μmol of

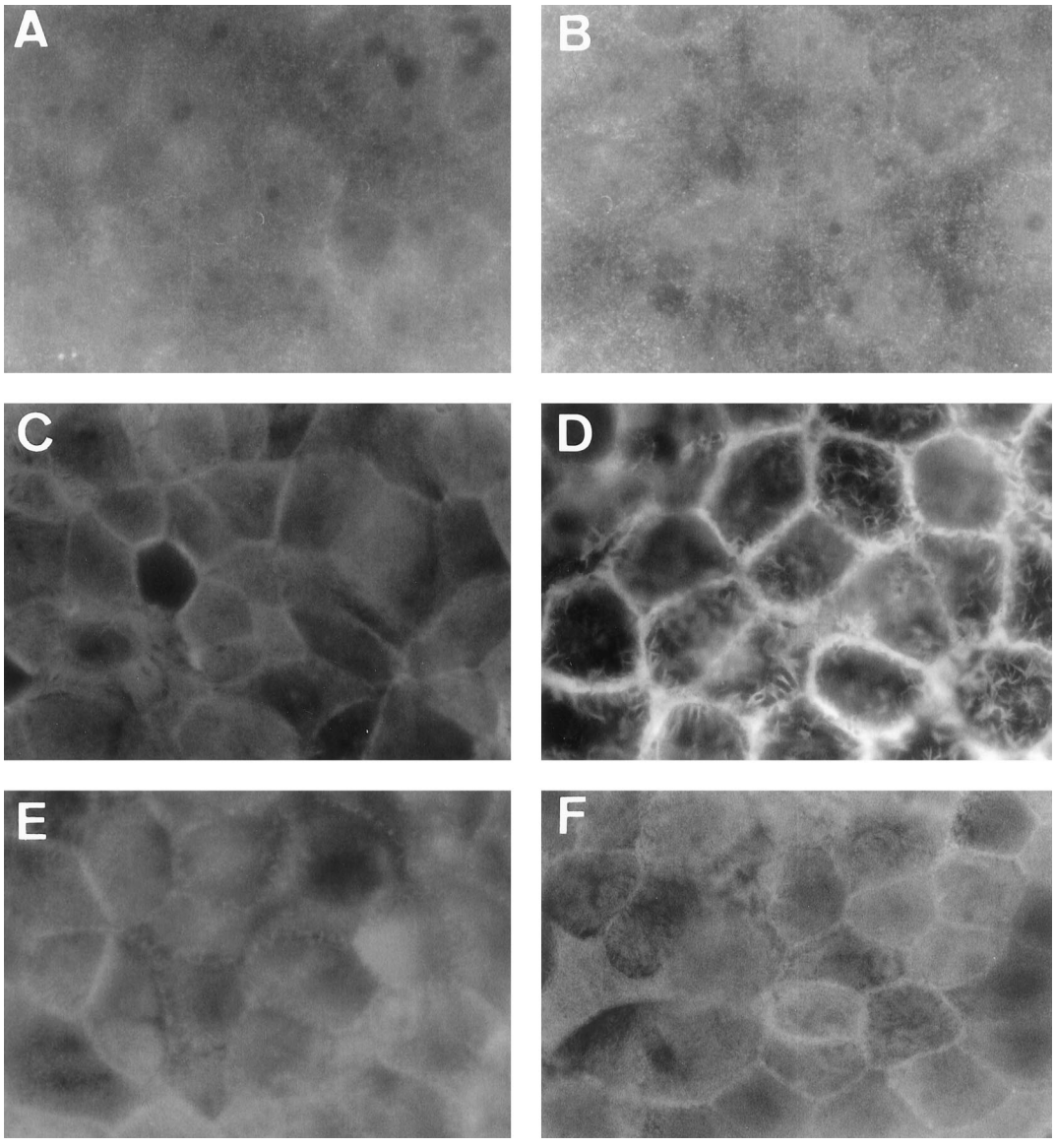

FIG. 1. Distribution of G- and F-actin and ADF in Afa/Dr DAEC C1845-infected cultured human polarized intestinal Caco-2/TC7 cells. Control (A, C, and E) and DAEC C1845-infected cells (B, D, and F) were stained with anti-G-actin polyclonal antibody (A and B), fluorescein-labeled phalloidin (F-actin labeling) (C and D), or anti-ADF polyclonal antibody (E and F). En face micrographs of control cells show the homogenous fine labeling of G-actin, F-actin, and ADF characteristic of brush border-associated proteins. The center regions of several cells seem to be unstained because the apical faces are convex and appear out of the focus. En face micrographs showing the immunolocalization of G-actin and ADF reveal that the homogenous immunolabeling of proteins is not modified in Afa/Dr DAEC C1845-infected cells. Immunolocalization of F-actin shows that the homogenous immunolabeling of protein is dramatically modified in Afa/Dr DAEC C1845-infected cells. Note that both the F-actin and ADF immunolabeling shows lateral concentrations at points of cell-to-cell contact. Magnifications, ×100.

substrate per min at 37°C. Proteins were determined by the bicinchoninic acid assay (Pierce Interchim, Montluçon, France).

Inhibitors. To examine the role of intracellular Ca^{2+} in DAEC C1845-induced F-actin disassembly, a blocker of Ca^{2+} release from the endoplasmic reticulum, dantrolene, was used. To chelate the intracellular Ca^{2+}, the cell-permeating Ca^{2+} chelator BAPTA/AM was used. Dantrolene in dimethyl sulfoxide or BAPTA/AM in methanol-dimethylformamide (50:50, vol/vol) was added to the culture medium 60 min before infection. All blockers were maintained during the infection time course (3 h). In a preliminary experiment, we selected for each inhibitor a range of concentrations showing no change in C1845 binding and apical F-actin network in noninfected control cells (not shown). Moreover, no change in cell and monolayer integrities was observed in uninfected cells treated with inhibitors by measuring LDH release and TER.

Statistics. Data are expressed as the mean ± SEM of several experiments, with at least three monolayers from three successive passages of cells per experiment. Statistical significance was assessed by Student's *t* test.

RESULTS

Afa/Dr DAEC infection in Caco-2/TC7 cells is followed by alteration in the distribution of brush border-associated cytoskeletal proteins. We have previously reported that in wild-type Afa/Dr DAEC C1845-infected Caco-2/TC7 cells, MV injuries develop (2). To explain how wild-type Afa/Dr DAEC C1845 infection promotes this cell injury, we conducted experiments in which distribution of brush border-associated proteins playing a pivotal role in brush border assembly was examined by either direct or indirect immunofluorescence labeling (Fig. 1 to 3). Cellular actin exists in two forms within polarized epithelial cells. A globular pool of monomeric actin

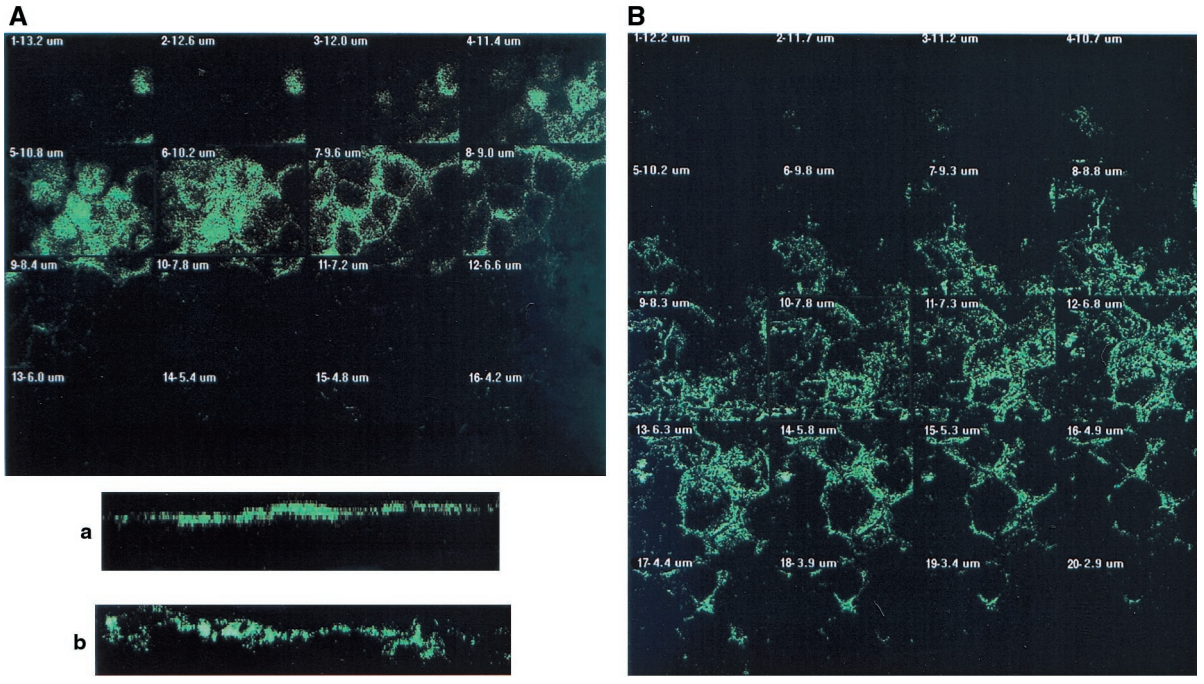

FIG. 2. CLSM analysis of F-actin immunolabeling in Afa/Dr DAEC C1845-infected Caco-2/TC7 cells. Confluent differentiated Caco-2/TC7 cells were infected apically at 37°C in a 10% CO_2–90% air atmosphere for 3 h with C1845 bacteria (10^8 CFU/well). Cells were fixed with 3.5% paraformaldehyde, washed, permeabilized with Triton X-100, and processed for immunofluorescence labeling as described in Materials and Methods. Fixed and permeabilized cells were processed for direct immunofluorescence labeling of F-actin with fluorescein-labeled phalloidin as described in Materials and Methods. Cells were examined using a confocal laser scanning microscope (model PCM 2000; Diaphot 300 microscope using a 100× Pan Fluor ELSW DM CF160 objective; Nikon). The samples were analyzed by serial optical horizontal sectioning. The section starts at the basal domain of the cells, and the following analysis was conducted until the apical domain was reached. (A and a) Control uninfected cells; (B and b) DAEC C1845-infected cells. (A and B) En face micrographs of the immunolocalization of F-actin obtained in CLSM analysis (horizontal *x-y* optical sections). In control cells, the majority of F-actin labeling starts on section 3 and afterwards is distributed in six sections (one section every 0.60 μm). In C1845-infected cells, the majority of the F-actin labeling starts on section 5 and afterwards is distributed in 12 sections (one section every 0.50 μm). (a and b) Lateral views of the immunolocalization of F-actin obtained in CLSM analysis (vertical *x-z* optical section). In control cells, F-actin labeling is localized at the apical domain in a homogenous band. In C1845-infected cells, apical F-actin labeling is dramatically modified, showing a disruption in apical labeling and delocalization of the protein in a nonhomogenous band.

(G-actin) is distributed diffusely throughout the cytoplasm. Oligomeric, polymerized, and filamentous actin (F-actin) are distributed in different cellular domains, including the terminal web and extending into the core of the MV. We performed an experiment in which indirect immunofluorescence localized these different forms of actin, and the analysis was conducted by confocal laser scanning microscopy (CLSM). En face micrographs focused at the apical domain show that in control Caco-2/TC7 cells expressing a well-organized brush border, immunolabeling using an MAb directed against G-actin (62) gives a diffuse staining pattern underneath the apical domain, typical of a cytoplasmic distribution (Fig. 1A). No change in G-actin distribution was found in C1845-infected cells (Fig. 1B). In control Caco-2/TC7 cells, the en face micrograph focused at the apical domain shows that direct labeling of F-actin with fluorescein-labeled phalloidin gives homogenous, fine, and flocculated labeling (Fig. 1C). This F-actin distribution is consistent with previous F-actin distribution centrally in the cells representing MV-associated F-actin, observed in clones or parental Caco-2 cells (11, 55, 57). In C1845-infected cells, the en face micrograph focused at the apical domain reveals that the homogenous apical F-actin labeling was dramatically altered, showing central lucent zones (Fig. 1D). It was noticed that F-actin disassembly develops as a function of both the multiplicity of infection and the time postinfection (not shown).

CLSM analysis was conducted from the apical to the basolateral domains of the cells to better examine the C1845-induced F-actin rearrangements (Fig. 2). In control cells, CLSM analysis (Fig. 2A) shows that F-actin was essentially localized at the apical domain and organized in a homogenous band of 3 μm (Fig. 2a). When we examined the distribution of F-actin in C1845-infected cells, we found that the immunolabeling was delocalized from the apical domain (Fig. 2B) and that a significant enlargement of the band (5.4 μm) was observed (Fig. 2b).

The assembly of the actin cytoskeleton depends upon the production and activities of a large number of actin-binding proteins (65). Among the most important of these proteins are the profilin, thymosin, and ADF/cofilin families, which have been implicated in regulating actin assembly in a number of different systems (for a review, see reference 64). ADF is a member of a 19-kDa family of calcium-independent, pH-sensitive, F-actin-binding/depolymerizing, and G-actin sequestering proteins (27). When examining ADF distribution by indirect immunofluorescence, we found that in control Caco-2/TC7 cells ADF shows diffuse staining throughout the cytoplasm of all the cells, consistent with ADF's being present in a detergent-soluble pool in brush border-forming cells (62). We observed no significant obvious change in ADF distribution in C1845-infected cells (Fig. 1E and F), suggesting that ADF is not involved in C1845-induced apical F-actin disassembly.

It is well known that cytoskeletal proteins such as villin play a pivotal role in brush border assembly and organization (for reviews, see references 28 and 39). The distribution of villin,

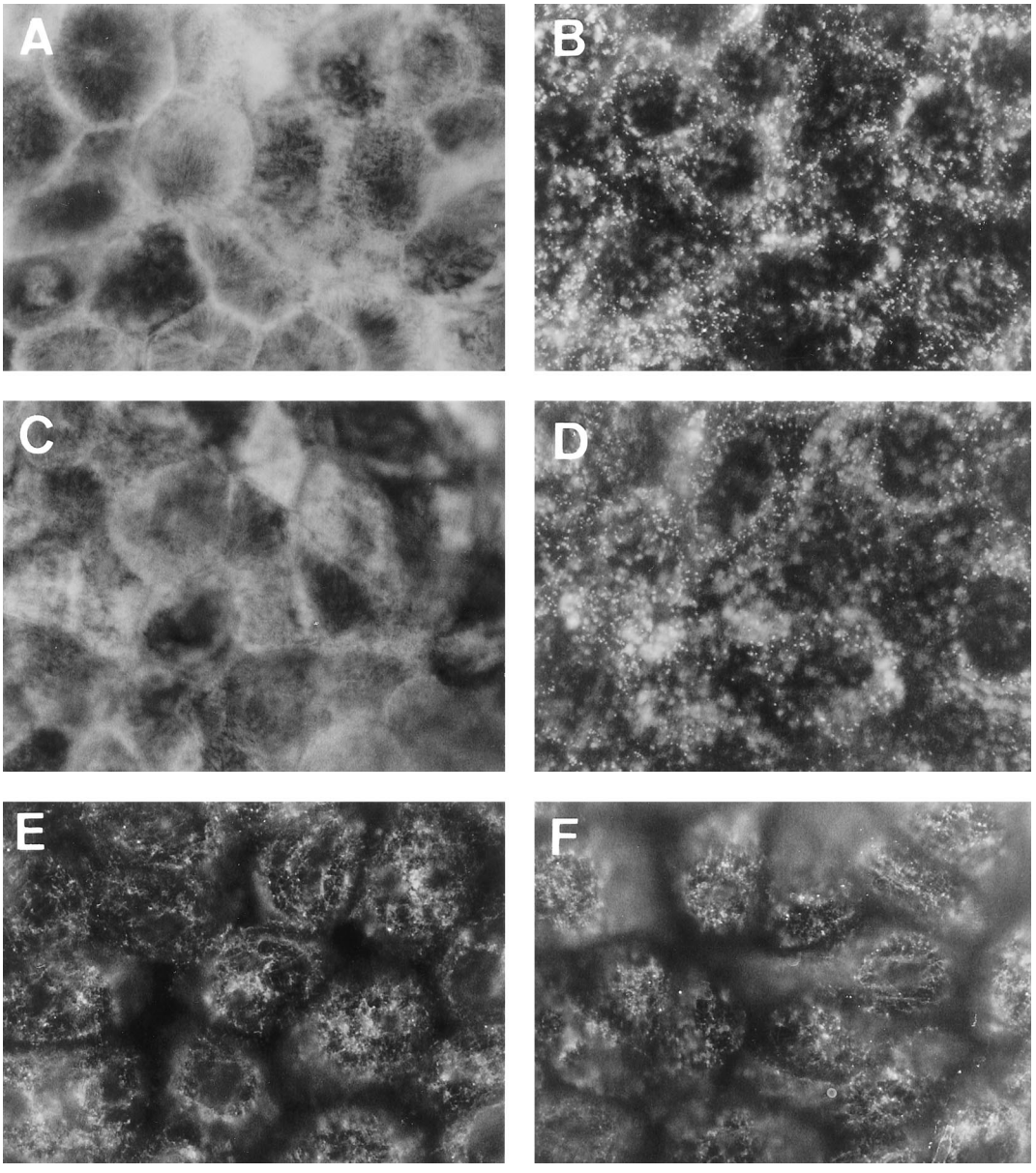

FIG. 3. Distribution of villin, fimbrin, and tubulin in Afa/Dr DAEC C1845-infected human cultured polarized intestinal Caco-2/TC7 cells. Experimental conditions were as in Fig. 1. Cells were stained with MAbs for antivillin (A and B), antifimbrin (C and D), and antitubulin (E and F). (A, C, and E) Control uninfected cells; (B, D, and F) DAEC C1845-infected cells. En face micrographs in control cells show the fine and homogenous labeling of villin and fimbrin characteristic of MV-associated proteins. The center regions of several cells seem to be unstained because the apical faces are convex and appear out of focus. In DAEC C1845-infected cells, disappearance of the fine and homogenous pattern and appearance of clusters of aggregated villin and fimbrin are observed. No change in tubulin distribution is observed DAEC C1845-infected cells. Magnifications, ×100.

fimbrin, spectrin, tropomyosin, and α-actinin was compared between uninfected and wild-type DAEC C1845-infected Caco-2/TC7 cells by indirect immunofluorescence (Fig. 3). Staining of both villin and fimbrin in Caco-2/TC7 cells was essentially localized to the apex of the cells since the fine, flocculated labeling centrally in the cells was characteristic of MV-associated proteins (Fig. 3A and C). In wild-type DAEC C1845-infected cells, there was a dramatic redistribution of both villin and fimbrin characterized by disappearance of the homogenous fine labeling and appearance of clumped proteins (Fig. 3B and D, respectively). This redistribution appears very different from the above-observed F-actin redistribution induced by wild-type DAEC C1845. When examining the situation of other brush border-associated cytoskeletal proteins such as spectrin, tropomyosin, and α-actinin, we found that their distribution was dramatically altered upon wild-type DAEC C1845 infection, being characterized again by disappearance of the fine labeling centrally in the cells and the appearance of randomly distributed small aggregates of clumped proteins (not shown). In contrast, no obvious abnormalities were found in the constitution of the microtubule network in wild-type C1845-infected Caco-2/TC7 cells (Fig. 3F) compared with microtubule organization in control cells (Fig. 3E).

Ca^{2+}-regulated events play a pivotal role in the assembly, organization, and maintenance of the brush border (7, 41, 45).

TABLE 1. Effect of calcium blockers on DAEC C1845-induced apical F-actin disassembly in Caco-2/TC7 cells[a]

Cells (treatment)	Concn (μM)	Mean relative F-actin immunofluorescence intensity ± SEM	Mean % of cells presenting apical F-actin disassembly ± SEM
Control		2.80 ± 0.18	0
Infected		0.32 ± 0.09	95 ± 5
Infected (BAPTA/AM)	7.5	1.12 ± 0.17*	60 ± 10*
	25	2.30 ± 0.19*	25 ± 5*
Infected (dantrolene)	100	0.75 ± 0.20*	75 ± 8*
	200	2.65 ± 0.35*	15 ± 6*

[a] Apical F-actin distribution was revealed by direct immunofluorescence labeling using phalloidin-fluorescein. Relative F-actin immunofluorescence intensity was reported as the mean ± SEM of arbitrary units measured as described in Materials and Methods. Results are also presented as the mean (± SEM) percentage of cells presenting apical F-actin disorganization relative to the total number of cells observed (54). Dantrolene and BAPTA/AM were present in the incubation medium 60 min before and during infection. Statistical analysis comparing infected cells with infected-treated cells was performed with a Student *t* test. *, significant difference ($P < 0.01$).

Rearrangements in MV-associated F-actin (6, 17, 64) through a Ca^{2+}-dependent mechanism have been reported, and this phenomenon could be antagonized by a chelator of intracellular Ca^{2+} (6). To document whether the DAEC C1845-induced apical cytoskeleton disassembly could result from Ca^{2+} signaling, we used both a blocker of intracellular Ca^{2+} release, dantrolene, and a chelator of intracellular Ca^{2+}, BAPTA/AM. We observed that both dantrolene and BAPTA/AM treatment blocked, identically and dose-dependently, DAEC C1845-induced apical F-actin disassembly (Table 1 and Fig. 4). This result suggests that a C1845-induced increase in intracellular calcium is necessary for F-actin disorganization.

The results reported above suggest that infection of Caco-2 cells by the wild-type Afa/Dr DAEC C1845 promotes a dedifferentiation of the apical domain of the polarized intestinal cells. We further conducted a transmission electron microscopy study to examine the morphological organization of the cells upon DAEC C1845 infection (Fig. 5). The uninfected Caco-2/TC7 cells are well polarized and display a continuous brush border composed of well-ordered and dense MV, which entirely carpet the apical surface (Fig. 5A and B). In contrast, the wild-type Afa/Dr DAEC C1845-infected Caco-2/TC7 cells show disappearance of the well-ordered MV. The remaining apical MV are dispersed (Fig. 5C), and the sparse MV are shortened but organized (Fig. 5D). It is of interest that despite the absence of a morphologically distinct brush border, the infected Caco-2/TC7 cells appeared to maintain the morphological organization characteristic of polarized epithelial cells (Fig. 5C). This was confirmed by observation that the cell and monolayer integrities, examined by measuring LDH release

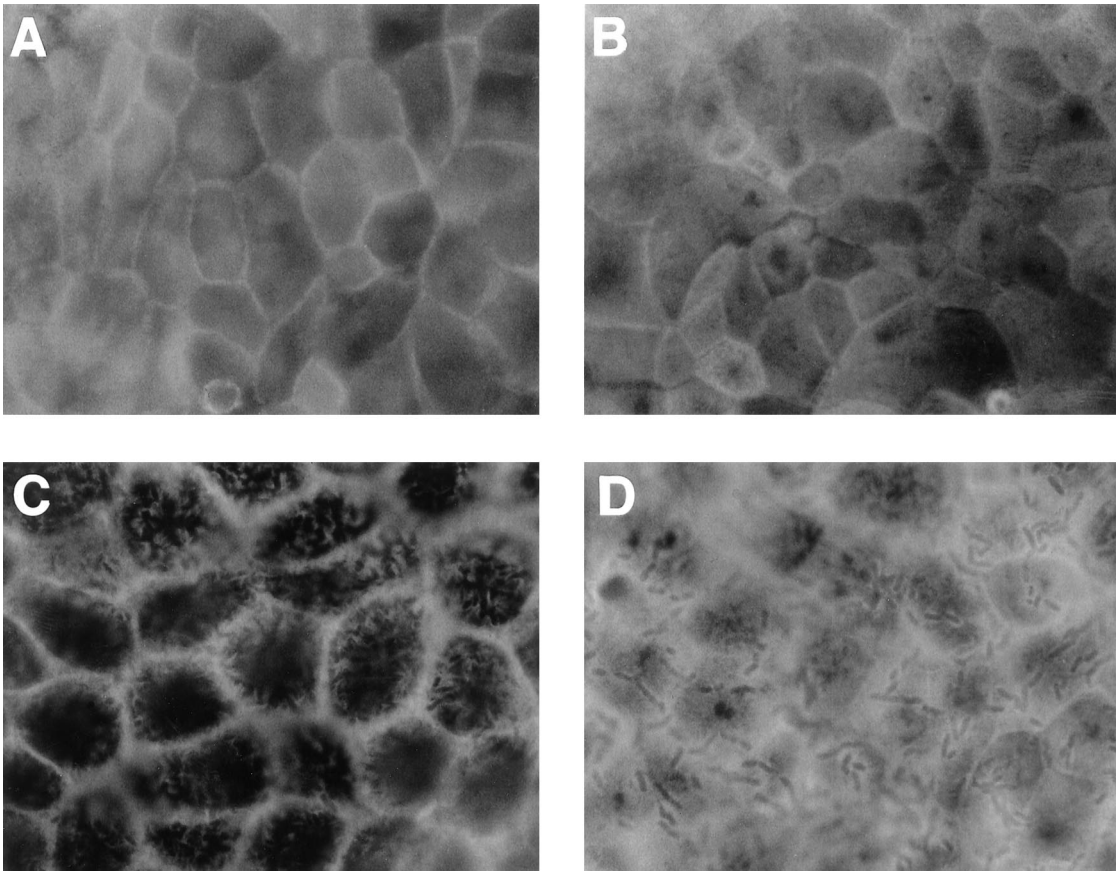

FIG. 4. Distribution of apical F-actin in Afa/Dr DAEC C1845-infected Caco-2/TC7 cells treated with the chelator of intracellular Ca^{2+} BAPTA/AM. Experimental conditions were as in Fig. 1. En face micrographs of the immunolocalization of apical F-actin in (A) uninfected control cells, (B) uninfected cells treated with BAPTA/AM (25 μM), (C) DAEC C1845-infected cells, and (D) DAEC C1845-infected cells treated with BAPTA/AM (25 μM). In DAEC C1845-infected cells treated with BAPTA/AM, the fine, flocculated F-actin labeling centrally in the cells remains present. Note that the adhering bacteria appeared at the cell surface and that F-actin organizes around the adhering bacteria. Magnifications, ×100.

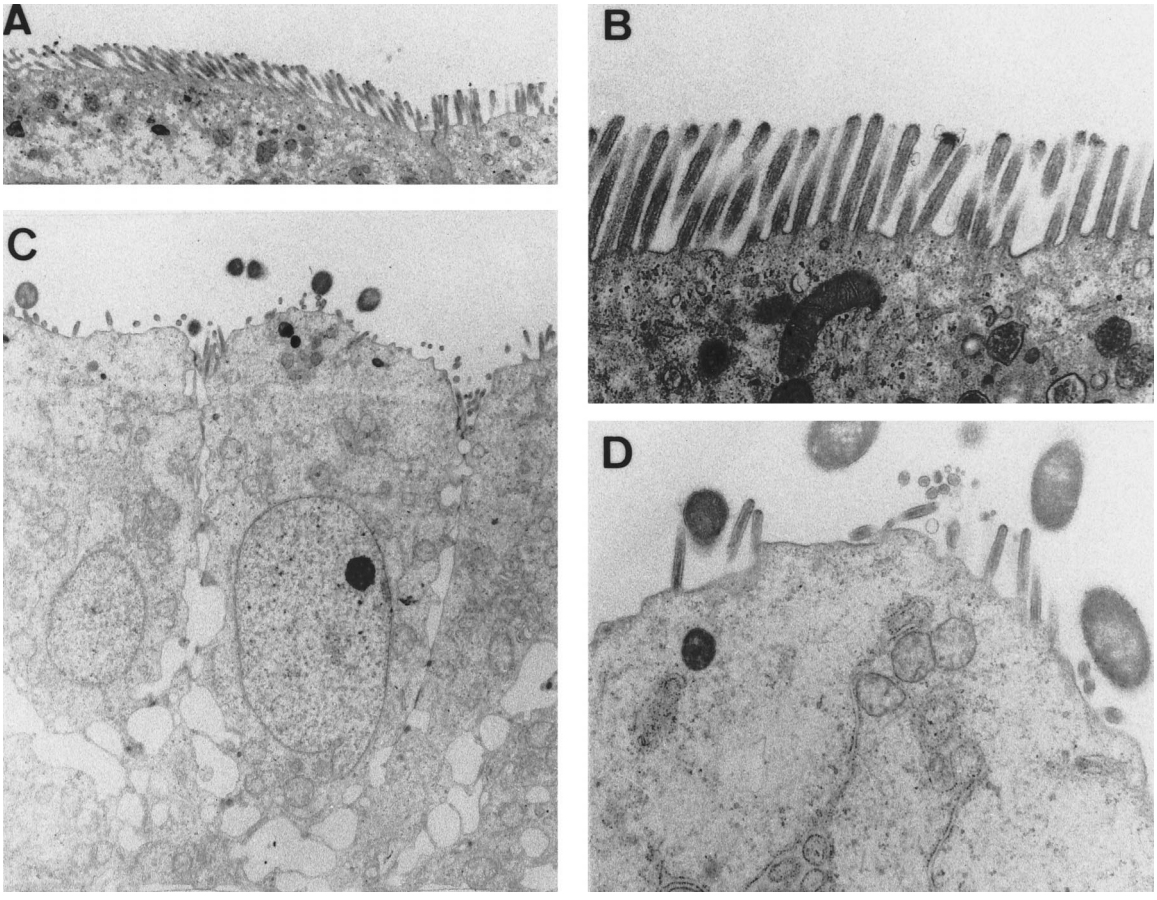

FIG. 5. Transmission electron microscopy of Afa/Dr DAEC C1845-infected Caco-2/TC7 cells shows the disappearance of the well-developed brush border. Experimental conditions were as in Fig. 1. (A and B) Transverse sections of the apical domain of uninfected Caco-2/TC7 cells at low and high magnifications, respectively. The apical domain of the polarized cells is uniformly organized, showing a continuous brush border with well-ordered and dense MV. (C and D) Transverse sections of the apical domain of Afa/Dr DAEC C1845-infected Caco-2/TC7 cells at low and high magnifications, respectively. The apical domain is rounded, with randomly distributed sparse and shortened MV. Note that the polarized organization of the infected cells is the same as that of uninfected cells. Low magnification, ×2,000; high magnification, ×5,000.

and TER, remained unchanged in infected cells. LDH release in control cells was 29 ± 5 U/ml and in infected cells was 29 ± 4 U/ml; in H_2O-lysed cells it was 4,272 ± 61. TER in control cells and infected cells was 883 ± 22 and 869 ± 24 Ω/cm^2, respectively.

Experiments conducted using the uropathogenic wild-type Afa/Dr DAEC strain IH11128 expressing the Dr hemagglutinin gave identical results (not shown). Taken together, these results indicate that infection of polarized intestinal cells by Afa/Dr DAEC is followed by cell injuries which result in a structural dedifferentiation of the apical domain of the cells.

Effect of point mutations in Dr hemagglutinin on Dr binding and Dr-induced F-actin disassembly in Caco-2/TC7 cells. Carnoy and Moseley (8) have recently observed that mutations at positions 32, 40, 54, 90, and 113 in Dr hemagglutinin cause different Afa/Dr phenotypes. We further investigated whether several of these point mutations could affect adhesin binding and F-actin rearrangements in Caco-2/TC7 cells (Table 2).

Dr^+ *E. coli* DH5α(pCC90), carrying the plasmid encoding the Dr hemagglutinin, bound efficiently to Caco-2/TC7 cells and promoted disassembly of apical F-actin. It was noticed that the DH5α(pCC90)-induced disassembly is less marked than that observed with the wild-type strain IH11128 expressing the Dr hemagglutinin. The insertion mutant *E. coli* BN17 (EC901[pBNJ17::Tn*3*]) (*draE*) and the *E. coli* mutant pCC90-

TABLE 2. Effect of point mutations within Dr hemagglutinin on binding and apical F-actin disassembly in Caco-2/TC7 cells[a]

Plasmid	Binding[b] (mean % ± SEM)	Apical F-actin disorganization (mean relative fluorescence intensity ± SEM)
pCC90	5.5 ± 0.4	95 ± 4
pCC90-D54stop	0.7 ± 0.2*	0[d]
BN17 (*draE*)	0.5 ± 0.2*	0[d]
pCC90-D54V	5.1 ± 0.5	96 ± 4
pCC90-D54Y	5.5 ± 0.2	95 ± 5
pCC90-T90M	5.8 ± 0.4	93 ± 8
pCC90-I113T	5.8 ± 0.5	93 ± 7
pCC90-D54G	2.0 ± 0.3*	15 ± 10*
pCC90-D54C	3.6 ± 0.5*	5 ± 4*

[a] Statistical analysis comparing pCC90 with the mutants was performed with a Student *t* test. *, Significant difference ($P < 0.01$).

[b] Percentage of ^{14}C-radiolabeled bacteria bound ± SEM.

[c] Apical F-actin organization was revealed by direct immunofluorescence labeling using phalloidin-fluorescein. Results are presented as the mean (± SEM) percentage of cells presenting apical F-actin disorganization relative to the total number of cells (54). Relative immunofluorescence intensities: uninfected cells, 2.78 ± 0.25; pCC90-infected cells, 0.42 ± 0.15; pCC90-D54G, 2.03 ± 0.40*; pCC90-D54C, 2.68 ± 0.30* (arbitrary units).

[d] Although *E. coli*(pCC90-D54stop) and BN17 (*draE*) did not adhere to Caco-2/TC7 cells, isolated adhering *E. coli* could be observed in randomly distributed cells without alteration of the apical F-actin network.

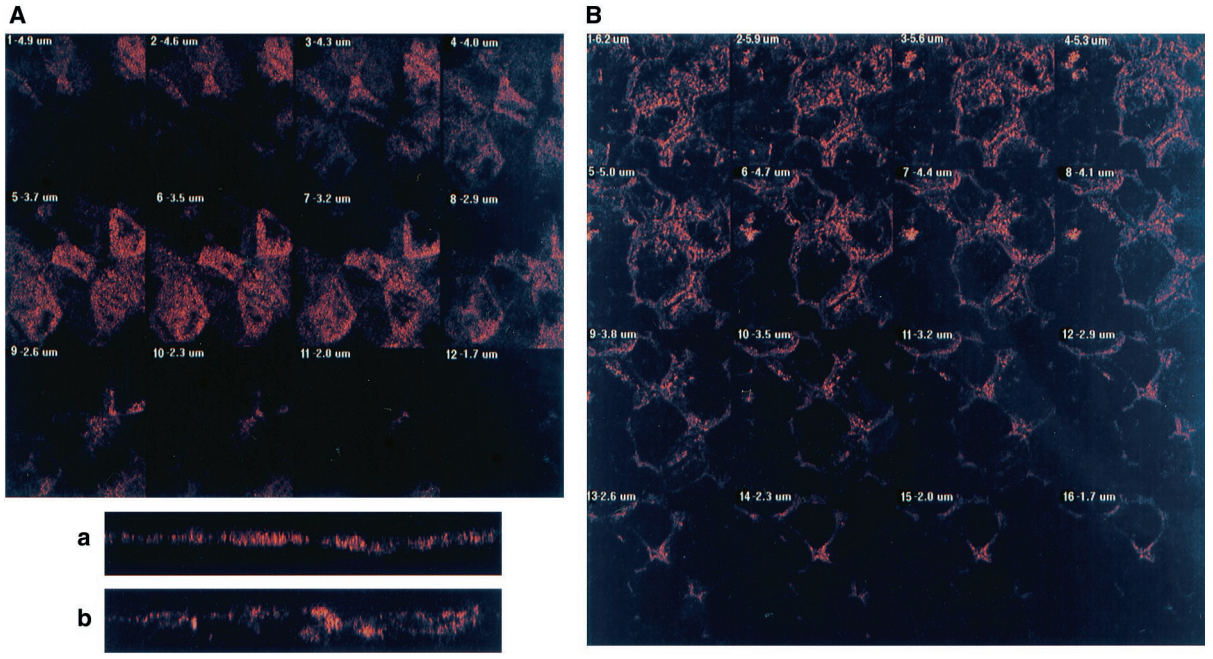

FIG. 6. CLSM analysis of SI immunolabeling in Afa/Dr DAEC C1845-infected Caco-2/TC7 cells shows a dramatic rearrangement of the brush border-associated hydrolase. Experimental conditions were as in Fig. 1. Cells were fixed with 3.5% paraformaldehyde, washed, and processed for indirect immunofluorescence labeling of SI as described in Materials and Methods. Cells were examined using a confocal laser scanning microscope (model PCM 2000; Nikon). The samples were analyzed by serial optical horizontal sectioning starting at the basal domain of the cells and following up to the apical domain. (A and a) Control uninfected cells; (B and b) DAEC C1845-infected cells. (A and B) En face micrographs of the immunolocalization of SI obtained in CLSM analysis (horizontal *x-y* optical sections). In control cells, the majority of the SI labeling starts on section 1 and afterwards is distributed in six successive sections (one section every 0.30 μm). In C1845-infected cells, the majority of the SI labeling starts on section 1 and afterwards is distributed in 11 sections (one section every 0.30 μm). (a and b) Lateral views of the immunolocalization of SI obtained in CLSM analysis (vertical *x-z* optical section). In control cells, SI labeling is restricted at the apical domain in a homogenous band. In C1845-infected cells, a profound rearrangement of the cell distribution of the brush border-associated hydrolase is observed. SI immunolabeling is dramatically modified, showing a disruption in its apical localization and the appearance of a nonhomogenous band, suggesting cytoplasmic redistribution.

D54stop lost adhesion to Caco-2/TC7 cells. It is interesting that when examining the randomly distributed Caco-2/TC7 cells to which a small number of pCC90-D54stop and BN17 *E. coli* mutants adhered, we found no alteration of the apical F-actin network. The mutants pCC90-T90M, pCC90-I113T, pCC90-D54V, and pCC90-D54Y retained the capacity to bind to Caco-2/TC7 cells and promoted F-actin disassembly. Mutant pCC90-D54G lost 64% of the binding to Caco-2/TC7 cells and entirely lost F-actin disassembly activity. Interestingly, mutant pCC90-D54C lost only 34% of the binding to Caco-2/TC7 cells, whereas it entirely lost F-actin disassembly activity.

Afa/Dr DAEC-induced cytoskeleton injuries are accompanied by impairments in functional brush border-associated proteins. Caco-2/TC7 cells express a brush border endowed with hydrolases SI and DPPIV (9), the Na^+-glucose cotransporter SGLT1 (40), and the fructose transporter GLUT5 (40). We examined the impact of infection by the wild-type strain C1845 on the distribution of these brush border-associated functional proteins by indirect immunofluorescence labeling. Specific antibodies were applied to fixed and nonpermeabilized cells, allowing us to detect functional proteins present within the apical cell membrane.

To better examine the rearrangement in SI distribution upon C1845 infection, a CLSM analysis was performed. Consistent with the known insertion of SI in the brush border membrane of epithelial cells of the small intestine and with its status as an apical marker of fully differentiated brush border cells (26, 56), examination of SI immunolabeling (Fig. 6 and Table 3) in control Caco-2/TC7 cells shows that the expression of SI was localized at the apical surface of the cells. Indeed, CLSM analysis shows that SI distributes in a homogenous band of 1.8 μm (Fig. 6A and a). In C1845-infected cells, CLSM analysis reveals that SI distribution is profoundly disorganized (Fig. 6). SI immunolabeling was nonhomogenous showing large lucent zones and a significant enlargement of the band

TABLE 3. Effect of infection by wild-type Afa/Dr DAEC strains C1845 and IH11128 on apical distribution and enzyme activity of brush border-associated hydrolases[a]

Enzyme	Cells	Mean relative immunofluorescence intensity ± SEM	Mean enzyme sp act (mU/mg of protein) ± SD (% inhibition)
SI	Controls	2.78 ± 0.32	135 ± 10
	C1845 infected	0.40 ± 0.14*	35 ± 15** (74)
	IH11128 infected	0.55 ± 0.20*	50 ± 20** (63)
DPPIV	Controls	1.80 ± 0.25	172 ± 7
	C1845 infected	1.25 ± 0.15*	124 ± 6* (28)
	IH11128 infected	1.30 ± 0.10*	123 ± 12* (28)

[a] Apical SI and DPPIV distribution was observed by indirect immunolabeling as described in Materials and Methods. Relative immunofluorescence intensity is reported as the mean ± SEM (arbitrary units). SI and DPPIV enzyme activities were determined on the total membrane fraction from control and infected (3 h postinfection) cells as described in Materials and Methods. Results are means ± standard deviation for five independent experiments conducted with successive cell passages. Percent inhibition of enzyme activity in infected cells calculated relative to enzyme activity in control cells is shown in parentheses. Statistical analysis comparing infected with control cells was performed with a Student *t* test. Significant difference: *, $P < 0.05$; **, $P < 0.01$.

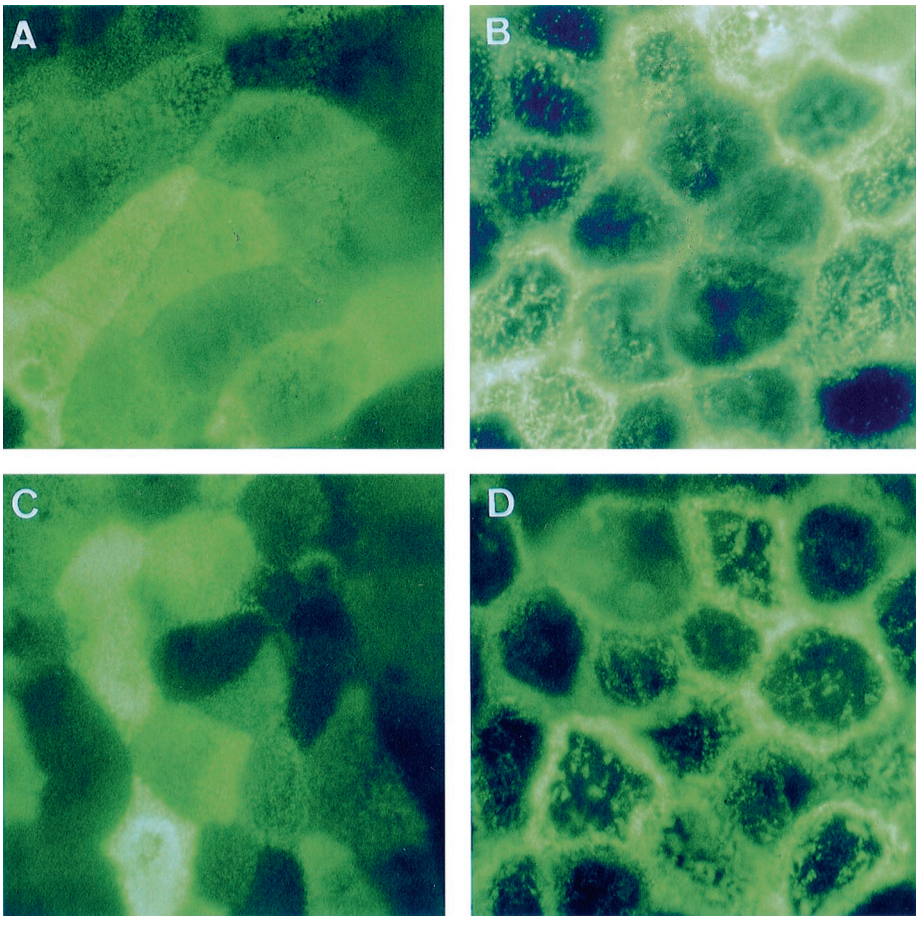

FIG. 7. Distribution of carbohydrate transporters GLUT5 and SGLT1 on Caco-2/TC7 cells infected by the wild-type Afa/Dr DAEC strain C1845. Experimental conditions were as in Fig. 1. The cells were stained with the appropriate MAbs directed against GLUT5 (A and B) or SGLT1 (C and D). (A and C) Control uninfected cells; (B and D) DAEC C1845-infected cells. En face micrographs of the immunolocalization of GLUT5 and SGLT1 in control cells (A and C) show the typical mosaic pattern distribution characteristic of MV-associated functional proteins. In C1845-infected cells (B and D), the mosaic pattern of distribution disappears. Note that clusters of aggregated proteins were observed centrally in the cells and that lateral concentrated immunolabeling at points of cell-to-cell contact underlined the honeycomb organization of the cells. Magnifications, ×100.

when SI was present (band of 3.3 μm) (Fig. 6A and b). When we examined the distribution of DPPIV in C1845-infected cells, we found an identical disorganization of its apical distribution (Table 3).

Examination of the apical distribution of fructose GLUT5 and glucose SGLT1 transporters was conducted (Fig. 7). In control Caco-2/TC7 cells, examination of GLUT5 and SGLT1 immunolabeling reveals the typical mosaic pattern of distribution of MV-associated functional proteins (Fig. 7A and C, respectively). This distribution results from the presence of a nonhomogenous organization of MV at the apical surface of the cells, i.e., cells with well-ordered MV and cells with dense and packed MV (55, 57). Moreover, the mosaic pattern results from the fact that the level of brush border-associated functional protein expression could vary from one cell to another (56). When the cells were infected by the Afa/Dr DAEC strain C1845, the mosaic pattern of GLUT5 and SGLT1 distribution disappeared (Fig. 7B and D, respectively). Large lucent zones centrally in the cells and clumped proteins were observed. In parallel, an intense labeling with a honeycomb-like organization localized at the cell-to-cell contact appeared.

The above results showing that apical distribution of SI and DPPIV is rearranged upon C1845 infection leads to the question of how the enzyme activity of these hydrolases evolves. In order to document this point, we determined the enzyme activity of SI and DPPIV in control and infected cells. Activity was measured only in a cell homogenate, since hydrolases in Caco-2 cells were not distributed between different cellular compartments but were mainly associated with the brush border (68). Infection of the cells by strain C1845 results in a dramatic decrease in SI enzyme activity and a lesser decrease in DPPIV enzyme activity (Table 3). A similar decrease in SI and DPPIV enzyme activities was observed in experiments conducted using the uropathogenic wild-type Afa/Dr DAEC strain IH11128 (Table 3).

DISCUSSION

Taken together, the results presented above indicated that infection of polarized intestinal cells by members of the Afa/Dr DAEC family is followed by cell injuries which result in structural and functional dedifferentiation of the apical domain of the cells. Many enteroadherent and enteroinvasive pathogens target the cytoskeleton in polarized epithelial cells, promoting development of diarrhea (for reviews, see references 47 and 63). Among the mechanisms by which a bacterial pathogen may colonize and disrupt intestinal function to cause malabsorption or diarrhea is bacterial attachment followed by local-

ized effacement of the epithelium. The best-demonstrated of these mechanisms of pathogenicity is that developed by enteropathogenic *E. coli* (EPEC). Contact of EPEC initiates localized adherence to the host cell receptor(s). This prerequisite event is followed by a complex pathway involving both secreted bacterial proteins and a complex of host cell signaling molecules necessary for focal actin cytoskeletal rearrangements and effacement of the MV. We have previously observed that Afa/Dr DAEC C1845 infection in Caco-2 cells is followed by a bacterial contact-dependent elongation of MV accompanied by vesiculation of the tips of MV which remained attached to the bacteria (2). Vesiculation of intestinal brush border MV accompanied by breakdown of the actin core bundle has been observed in the presence of high concentrations of Ca^{2+} (7, 41). In DAEC-infected HeLa cells, an increase in the intracellular Ca^{2+} concentration has been found to result from an influx of Ca^{2+} from the extracellular medium rather than Ca^{2+} mobilization from intracellular stores (31). Previously (54), we demonstrated that in Afa/Dr DAEC-infected cultured human intestinal cells, the induced F-actin disassembly results from calcium signaling events. It has recently been demonstrated that F-actin MV disassembly in Caco-2 cells following rotavirus infection (29) results from a rotavirus-induced increase in the intracellular concentration of Ca^{2+} (6). A Ca^{2+}-induced mechanism involving the breakdown of F-actin is known to be mediated by Ca^{2+}-dependent, actin-severing proteins, of which villin is available in the proximal tubule cells and absorptive cells of the small intestine (for reviews, see references 39 and 64). In the present study, our results bring new insights to explain the mechanism of pathogenicity of the Afa/Dr DAEC strains which promote a dramatic disappearance of the brush border accompanied by disorganization of the cytoskeleton proteins playing a pivotal role in the organization and maintenance of the brush border. When examining apical G- and F-actin distribution in infected polarized Caco-2/TC7 cells, we found no change in G-actin distribution, whereas apical F-actin disappears dramatically. Interestingly, we found that bacterial infection promotes the disassembly of both villin and fimbrin into globular forms. In the presence of a high concentration of Ca^{2+}, the severing activity of villin develops (5). Villin mediated a change in the state of actin polymerization and the spatial arrangement of actin protofilaments modulating the dynamics of the actin cytoskeleton. In particular, villin, which bundles, nucleates, caps, and severs actin in a Ca^{2+}-dependent manner in vitro, plays a major role in the organization and stabilization by lateral interactions of the brush border core bundle. The pivotal role of villin in MV assembly and brush border organization has been demonstrated in comprehensive and elegant studies. Costa de Beauregard et al. (11) have demonstrated that suppression of villin by antisense mRNA in Caco-2 cells impairs the formation of the brush border. Ferrary et al. (17) recently demonstrated that isolated intestinal brush borders of mice could be disrupted by the addition of Ca^{2+} or by increasing intracellular Ca^{2+} by serosal carbachol or mucosal Ca^{2+} ionophore A23187. To explain these brush border injuries, the authors suggested that villin could be the major cytoskeletal protein able to control Ca^{2+}-dependent actin fragmentation. Interestingly, as we have observed in Afa/Dr DAEC-infected Caco-2 cells, the Ca^{2+}-dependent disruption of F-actin in mouse brush border small intestine is specifically observed at the apical domain, since the basolateral F-actin was unaltered. Moreover, changes in Ca^{2+} in proximal tubule cells promote alterations of the MV actin cytoskeleton through a mechanism involving villin-mediated actin cytoskeletal disruption (64). It is tempting to speculate that the Afa/Dr DAEC-induced brush border injuries observed here and previously (2) result from Ca^{2+}-dependent villin disassembly, which would in turn induce disassembly of the apical F-actin.

When examining whether site-directed mutagenesis of the Dr hemagglutinin affected Afa/Dr DAEC F-actin rearrangements in Caco-2/TC7 cells, we found that when the aspartic acid residue at position 54 was replaced by cysteine, the mutant conserved a high capacity of binding but entirely lost the capacity to disassemble the apical F-actin. Interestingly, this mutant failed to induce the mobilization of CD66 and CD66e around adhering bacteria (24). Altogether, these results suggest that this point mutation in the Dr adhesin could promote a failure in adhesin-induced signaling (54) without affecting binding. The N-terminal 54 amino acids in Afa/Dr adhesins has been found to be involved in expression of Afa/Dr phenotypes. Carnoy and Moseley (8) have demonstrated that mutations at positions 32, 40, 54, 90, and 113 affected type IV collagen binding and chloramphenicol sensitivity of binding differently, while they had no effect on mannose-resistant hemagglutination. Le Bouguenec et al. (35), using strain A30 expressing the Afa-III adhesin, demonstrated that the aspartic acid residue located at the position 52 was associated with the chloramphenicol-sensitive hemagglutination phenotype.

Polarized cells enable epithelia to exert their most specialized roles, including absorption and secretion (for a review, see reference 16). The functionality of polarized epithelial cells depends on vesicular traffic and on the correct insertion of functional components in distinct plasma membrane domains. The apical domain facing the external compartment contains membrane-associated proteins such as enzymes, transporters, and ions, supporting specialized properties involved in the specific functions of absorption and secretion (for a review, see reference 39). The alteration in actin cytoskeleton, which regulates the function of many membrane-associated components linked within the specialized domains of epithelial cells, is the basis of disease processes (for a review, see reference 36). Our results showed that an alteration in the distribution of these brush border-associated functional proteins occurs upon infection by some wild-type Afa/Dr DAEC strains and was accompanied by a dramatic decrease in SI activity. It is tempting to speculate that the decrease in expression of brush border-associated functional proteins results from the Afa/Dr DAEC-induced cytoskeleton injuries. Indeed, cytoskeletal reorganization in polarized intestinal cells has been found to be accompanied by impairment of distribution of functional brush border-associated proteins. Stable expression of antisense villin RNA in Caco-2 cells, which impairs the brush border, alters expression of the functional intestinal hydrolase SI (11). The downregulation of cytokeratin 19 in Caco-2 cells resulted in a decrease in the number of MV, disorganization of the apical but not lateral or basal filamentous actin, and depletion or redistribution of apical membrane-associated proteins such as SI and alkaline phosphatase (61). It has been reported that MV atrophy is a distinct disorder within the syndrome of intractable diarrhea of infancy (13, 14, 60). Morphologically, there is a loss of villi, with enterocytes showing scanty, disorganized, and short MV. These structural injuries were accompanied by substantially reduced unidirectional absorptive and secretory fluxes of sodium and chloride, with net secretion of both, a decrease in disaccharidase activities, and abnormal glucose absorption. Our present and previous observations (2) showing that the Caco-2 cell brush border is dramatically impaired upon wild-type Afa/Dr DAEC C1845 infection, suggest that the diarrhea induced by this pathogen could result from a deficit in functional brush border-associated systems controlling the absorption and secretion function. Epidemiological reports indicated that EPEC and enteroaggregative *E. coli* strains are a significant cause of protracted diarrhea in children (for a review, see reference 20). Interestingly, epide-

miological studies have established a link between DAEC and persistent diarrheal diseases, mostly in infants older than 24 months (1, 21, 25, 37).

Some Afa/Dr DAEC strains infect the urogenital tract (for a review, see reference 15). Indeed, the cells lining the urogenital tract express the CD55 molecule, the receptor for Afa/Dr DAEC (49, 53). Complement-regulatory proteins are involved in glomerular diseases (46). Consistent with Dr hemagglutinin binding (48) on functional sites of the complement-regulatory CD55 molecule (12), it has been postulated that Afa/Dr DAEC uropathogens lead to immunopathological lesions. In an experimental mouse model of ascending pyelonephritis, Nowicki and colleagues (22, 52) recently demonstrated that infection by the Afa/Dr DAEC strain IH11128 leads to significant histological changes corresponding to tubulointerstitial nephritis, including interstitial inflammation, fibrosis, and tubular atrophy. Our results indicated that another mechanism of pathogenicity could be developed by Afa/Dr DAEC in the urogenital tract. Indeed, the observation that the uropathogenic Afa/Dr DAEC strain IH11128 has the same mechanism of pathogenicity as the diarrheagenic strain C1845 is of interest. Indeed, there are structural similarities between renal and intestinal polarized epithelial cells expressing a brush border and forming an epithelial barrier. Uroepithelial cells expressed apical MV supporting specialized functions, several of them being identical to those of intestinal cells. Moreover, villin has been shown to be an early marker of the proximal tubule cell lineage (42). Recent reports have found that MV damage in proximal tubule cells results from Ca^{2+}-dependent cytoskeleton disruption (43, 44, 64). Considering this and the results reported here showing that the uropathogenic Afa/Dr DAEC strain IH11128 rearranges brush border-associated cytoskeletal proteins by activation of CD55-associated signaling, it is tempting to speculate that uropathogenic Afa/Dr DAEC strains could promote kidney injuries through the induced cytoskeletal lesions.

In conclusion, our work demonstrates that infection of polarized human intestinal cells by Afa/Dr DAEC strains is followed by brush border injuries resulting from the Ca^{2+}-dependent disassembly of cytoskeletal proteins playing a pivotal role in brush border assembly. These structural injuries were accompanied in turn by a dramatic modification in distribution and enzyme activity of functional intestinal proteins. Altogether, these results give new insights on the mechanism by which the Afa/Dr DAEC could promote persistent diarrhea in children.

ACKNOWLEDGMENTS

We are grateful to D. Louvard, M. Arpin, and S. Robine for the generous gift of fimbrin and villin antibodies. We thank E. Brot-Laroche for the generous gift of anti-GLUT5 and anti-SGLT1 antibodies. We thank J. Bamburg for the gift of ADF antibody. We thank G. Delrue (INSERM SC6) for his skills in producing the art drawings.

J. Guignot is supported by a doctoral fellowship from the Ministère de l'Education Nationale, de la Recherche et de la Technologie (MENRT). C. Carnoy is supported by a grant from the Délégation à la Recherche (CHRU Lille). A. L. Servin is supported for this work by a grant from the Programme de Recherche Fondamentale en Microbiologie et Maladies Infectieuses et Parasitaires (PRFIMMIP-MENRT). S. L. Moseley is supported for this work by grant DK49862 from the National Institute of Diabetes and Digestive and Kidney Diseases. B. J. Nowicki is supported for this work by grant DK42029 from the NIDDK.

REFERENCES

1. **Baqui, A. H., R. B. Sack, R. E. Black, K. Haider, A. Hossain, A. R. Alim, M. Yunus, H. R. Chowdhury, and A. K. Siddique.** 1992. Enteropathogens associated with acute and persistent diarrhea in Bangladeshi children less than 5 years of age. J. Infect. Dis. **166:**792–796.
2. **Bernet-Camard, M.-F., M.-H. Coconnier, S. Hudault, and A. L. Servin.** 1996. Pathogenicity of the diffusely adhering strain *Escherichia coli* C1845: F1845 adhesin-decay accelerating factor interaction, brush border microvillus injury, and actin disassembly in cultured human intestinal epithelial cells. Infect. Immun. **64:**1818–1828.
3. **Bilge, S. S., J. M. Apostol, Jr., K. J. Fullner, and S. L. Moseley.** 1993. Transcriptional organization of the F1845 fimbrial adhesin determinant of *Escherichia coli*. Mol. Microbiol. **7:**993–1006.
4. **Bilge, S. S., C. R. Clausen, W. Lau, and S. L. Moseley.** 1989. Molecular characterization of a fimbrial adhesin, F1845, mediating diffuse adherence of diarrhea-associated *Escherichia coli* to HEp-2 cells. J. Bacteriol. **171:**4281–4289.
5. **Bretscher, A., and K. Weber.** 1980. Villin is a major protein of the microvillus cytoskeleton which binds both G and F actin in a calcium-dependent manner. Cell **20:**839–847.
6. **Brunet, J.-P., J. Cotte-Laffitte, C. Linxe, A.-M. Quéro, M. Géniteau Legendre, and A. L. Servin.** 2000. Rotavirus infection induces an increase in intracellular calcium concentration in human intestinal epithelial cells: role in microvillar actin alteration. J. Virol., **74:**2323–2332.
7. **Burgess, D. R., and B. E. Prum.** 1982. Reevaluation of brush border motility: calcium induces core filament isolation and microvillar vesiculation. J. Cell Biol. **94:**97–107.
8. **Carnoy, C., and S. L. Moseley.** 1997. Mutational analysis of receptor binding mediated by the Dr family of *Escherichia coli* adhesins. Mol. Microbiol. **23:**365–379.
9. **Chantret, I., A. Rodolosse, A. Barbat, E. Dussault, E. Brot-Laroche, A. Zweibaum, and M. Rousset.** 1994. Differential expression of sucrase-isomaltase in clones isolated from early and late passages of the cell line Caco-2: evidence for glucose-dependent negative regulation. J. Cell Sci. **107:**213–225.
10. **Cookson, S. T., and J. P. Nataro.** 1996. Characterization of Hep-2 cell projection formation induced by diffusely adherent *Escherichia coli*. Microb. Pathog. **21:**421–434.
11. **Costa de Beauregard, M. A., E. Pringault, S. Robine, and D. Louvard.** 1995. Suppression of villin expression by antisense RNA impairs brush border assembly in polarized epithelial intestinal cells. EMBO J. **14:**409–442.
12. **Coyne, K. E., S. E. Hall, E. S. Thompson, M. A. Acre, T. Kinoshita, T. Fujita, D. J. Anstee, W. Rosse, and D. M. Lublin.** 1992. Mapping epitopes, glycosylation sites, and complement regulatory domains in human decay accelerating factor. J. Immunol. **149:**2906–2913.
13. **Cutz, E., J. M. Rhoads, B. Drumm, P. M. Sherman, P. R. Durie, and G. G. Forstner.** 1989. Microvillus inclusion disease: an inherited defect of brush-border assembly and differentiation. N. Engl. J. Med. **9:**646–651.
14. **Davidson, G. P., E. Cutz, J. R. Hamilton, and D. G. Gall.** 1978. Familial enteropathy: a syndrome of protracted diarrhea from birth, failure to thrive, and hypoplastic villus atrophy. Gastroenterology **75:**783–790.
15. **D'Orazio, S. E. F., and C. M. Collins.** 1998. Molecular pathogenesis of urinary tract infections. Curr. Top. Microbiol. Immunol. **225:**137–164.
16. **Fath, K. R., S. N. Mamajiwalla, and D. R. Burgess.** 1993. The cytoskeleton in development of epithelial polarity. J. Cell Sci. **17:**65–73.
17. **Ferrari, E., M. Cohen-Tannouji, G. Pehau-Arnaudet, A. Lapillonne, R. Athman, T. Ruiz, L. Boulouha, F. El Marjou, A. Doye, J.-J. Fontaine, C. Antony, C. Babinet, D. Louvard, F. Jaisser, and S. Robine.** 1999. In vivo, villin is required for Ca^{2+}-dependent F-actin disruption in intestinal brush border. J. Cell Biol. **23:**819–829.
18. **Garcia, M. I., P. Gounon, P. Courcoux, A. Labigne, and C. Le Bouguenec.** 1996. The afimbrial adhesive sheath encoded by the afa-3 gene cluster of pathogenic *Escherichia coli* is composed of two adhesins. Mol. Microbiol. **19:**683–693.
19. **Garcia, M. I., A. Labigne, and C. Le Bouguenec.** 1994. Nucleotide sequence of the afimbrial adhesin-encoding *afa-3* gene cluster and its translocation via flanking IS*1* insertion sequences. J. Bacteriol. **76:**7601–7613.
20. **Garcia, M. I., and C. Le Bouguenec.** 1996. Role of adhesion in pathogenicity of human uropathogenic and diarrhoeogenic *Escherichia coli*. Bull. Inst. Pasteur **94:**201–236.
21. **Giron, J. A., T. Jones, F. Millan Velasco, E. Castro Munoz, L. Zarate, J. Fry, G. Frankel, S. L. Moseley, B. Baudry, J. B. Kaper, G. K. Schoolnick, and L. W. Riley.** 1991. Diffuse-adhering *Escherichia coli* (DAEC) as a putative cause of diarrhea in Mayan children in Mexico. J. Infect. Dis. **163:**507–513.
22. **Goluszko, P., S. L. Moseley, L. D. Truong, A. Kaul, J. R. Williford, R. Selvarangan, S. Nowicki, and B. Nowicki.** 1997. Development of experimental model of chronic pyelonephritis with *Escherichia coli* O75:K5:H-bearing Dr fimbriae: mutation in the *dra* region prevented tubulointerstitial nephritis. J. Clin. Investig. **99:**1662–1672.
23. **Goluszko, P., R. Selvarangan, V. Popov, T. Pham, J. W. Wen, and J. Singhal.** 1999. Decay-accelerating factor and cytoskeleton redistribution pattern in HeLa cells infected with recombinant *Escherichia coli* strains expressing Dr family of adhesins. Infect. Immun. **67:**3989–3997.
24. **Guignot, J., I. Peiffer, M. F. Bernet-Camard, D. Lublin, C. Carnoy, S. L. Moseley, and A. L. Servin.** 2000. Recruitment of CD55 and CD66e brush border-associated glycosylphosphatidylinositol-anchored proteins by mem-

bers of the Afa/Dr diffusely adhering *Escherichia coli* family infecting the human polarized intestinal Caco-2/TC7. Infect. Immun. **68:**3554–3563.
25. **Gunzberg, S. T., B. J. Chang, S. J. Elliot, V. Burke, and M. Gracey.** 1993. Diffuse and enteroaggregative patterns of adherence of enteric *Escherichia coli* isolated from aboriginal children from the Kimberley region of western Australia. J. Infect. Dis. **167:**755–758.
26. **Hauri, H. P., E. E. Sterchi, D. Bienz, J. A. M. Fransen, and A. Marxer.** 1985. Expression and intracellular transport to microvillus membrane hydrolases in human intestinal epithelial cells. J. Cell Biol. **101:**838–851.
27. **Hayden, S. M., P. S. Miller, A. Brauweiler, and J. R. Bamburg.** 1993. Analysis of the interactions of actin depolimerizing factor with G- and F-actin. Biochemistry **32:**9994–10004.
28. **Heintzelman, M. B., and M. S. Mooseker.** 1992. Assembly of the intestinal brush border cytoskeleton. Curr. Top. Dev. Biol. **26:**93–122.
29. **Jourdan, N., J.-P. Brunet, C. Sapin, A. Blais, A.-M. Quéro, G. Trugnan, and A. L. Servin.** 1998. Rotavirus infection reduces sucrase-isomaltase expression in human intestinal epithelial cells by perturbing protein targeting and organization of microvillar cytoskeleton. J. Virol. **72:**7228–7236.
30. **Jouve, M., M. I. Garcia, P. Courcoux, A. Labigne, P. Gounon, and C. Le Bouguenec.** 1997. Adhesion to and invasion of HeLa cells by pathogenic *Escherichia coli* carrying the *afa-3* gene cluster are mediated by the AfaE and AfaD proteins, respectively. Infect. Immun. **65:**4082–4089.
31. **Karmaker, S., A. G. Chaudhuri, and U. Ganguly.** 1996. Comparison of cytosolic levels of calcium and G actin in diffuse and localised adherent *Escherichia coli*-infected HeLa cells. FEMS Microbiol. Lett. **135:**245–249.
32. **Kernéis, S., M.-F. Bernet, J.-M. Gabastout, M.-H. Coconnier, B. J. Nowicki, and A. L. Servin.** 1994. Human cultured intestinal cells express attachment sites for uropathogenic *Escherichia coli* bearing adhesins of the Dr adhesin family. FEMS Microbiol. Lett. **119:**27–32.
33. **Kernéis, S., S. S. Bilge, V. Fourel, G. Chauvière, M.-H. Coconnier, and A. L. Servin.** 1991. Use of purified F1845 fimbrial adhesin to study localization and expression of receptors for diffusely adhering *Escherichia coli* during enterocytic differentiation of human colon carcinoma cell lines HT-29 and Caco-2 in culture. Infect. Immun. **59:**4013–4018.
34. **Labigne-Roussel, A., M. A. Schmidt, W. Waltz, and S. Falkow.** 1985. Genetic organization of the afimbrial adhesin operon and nucleotide sequence from a uropathogenic *Escherichia coli* gene encoding an afimbrial adhesin. J. Bacteriol. **162:**1285–1292.
35. **Le Bouguenec, C., M. I. Garcia, V. Ouin, J. M. Desperrier, P. Gounon, and A. Labigne.** 1993. Characterization of plasmid-borne *afa-3* gene clusters encoding afimbrial adhesins expressed by *Escherichia coli* strains associated with intestinal or urinary tract infections. Infect. Immun. **61:**5106–5114.
36. **Leiser, J., and B. A. Molitoris.** 1993. Disease processes in epithelia: the role of the actin cytoskeleton and altered surface membrane polarity. Biochem. Biophys. Acta **1225:**1–13.
37. **Levine, M. M., C. Ferreccio, V. Prado, M. Cayazzo, P. Abrego, and J. Martinez, L. Maggi, M. M. Baldini, W. Martin, D. Maneval, B. Kay, L. Guers, H. Lior, S. S. Watermann, and J. P. Nataro.** 1993. Epidemiologic studies of *Escherichia coli* diarrheal infections in a low socioeconomic level peri-urban community in Santiago, Chile. Lancet **i:**1119–1122.
38. **Loomis, W. P., and S. L. Moseley.** 1998. Translational control of mRNA processing in the F1845 fimbrial operon of *Escherichia coli*. Mol. Microbiol. **30:**843–853.
39. **Louvard, D., M. Kedinger, and H. P. Hauri.** 1992. The differentiating intestinal epithelial cell: establishment and maintenance of functions through interactions between cellular structures. Annu. Rev. Cell Biol. **8:**157–195.
40. **Mahraoui, L., A. Rodolosse, A. Barbat, E. Dussaulx, A. Zweibaum, M. Rousset, and E. Brot-Laroche.** 1994. Presence and differential expression of SGLT1, GLUT1, GLUT2, GLUT3 and GLUT5 hexose-transporter mRNAs in Caco-2 cell clones in relation to cell growth and glucose consumption. Biochem. J. **298:**629–633.
41. **Matzudaira, P. T., and D. R. Burgess.** 1982. Organization of the cross-filaments in intestinal microvilli. J. Cell Biol. **92:**657–664.
42. **Maunoury, R., S. Robine, E. Pringault, N. Léonard, J. A. Gaillard, and D. Louvard.** 1992. Development of villin gene expression in the epithelial cell lineages of mouse digestive and urogenital tracts. Development **115:**717–728.
43. **Molitoris, B. A., R. Dahl, and M. Hisford.** 1996. Cellular ATP depletion induces disruption of the spectrin cytoskeletal network. Am. J. Physiol. **271:**F790–F798.
44. **Molitoris, B. A., A. Geerdes, and J. R. McIntosh.** 1991. Dissociation and redistribution of Na^+K^+-ATPase from its surface membrane actin cytoskeletal complex during cellular ATP depletion. J. Clin. Investig. **88:**462–469.
45. **Mooseker, M. S., T. A. Graves, K. A. Wharton, N. Falco, and C. L. Howe.** 1980. Regulation of microvillus structure: calcium-dependent solation and cross-linking of actin filaments in the microvilli of intestinal epithelial cells. J. Cell Biol. **87:**809–822.
46. **Nangaku, M.** 1998. Complement regulatory proteins in glomerular diseases. Kidney Int. **54:**1419–1428.
47. **Nataro, J. P., and J. B. Kaper.** 1998. Diarrheagenic *Escherichia coli*. Clin. Microbiol. Rev. **11:**403–503.
48. **Nowicki, B., A. Hart, K. E. Coyne, D. M. Lublin, and S. Nowicki.** 1993. Short consensus repeat-3 domain of recombinant decay-accelerating factor is recognized by *Escherichia coli* recombinant Dr adhesin in a model of cell-cell interaction. J. Exp. Med. **178:**2115–2121.
49. **Nowicki, B., H. Holthofer, and T. Savarena.** 1986. Location of adhesion sites for P fimbriated and for O75X-positive *Escherichia coli* in the human kidney. Microb. Pathog. **1:**169–180.
50. **Nowicki, B., A. Labigne, S. Moseley, R. Hull, S. Hull, and J. Moulds.** 1990. The Dr hemagglutinin, afimbrial adhesins AFA-I, AFA-II, and AFA-II, and F1845 fimbriae of uropathogenic and diarrhea-associated *Escherichia coli* belong to a family of hemagglutinins with the Dr receptor recognition. Infect. Immun. **58:**279–281.
51. **Nowicki, B., J. Moulds, R. Hull, and S. Hull.** 1988. A hemagglutinin of uropathogenic *Escherichia coli* recognizes the Dr blood group antigen. Infect. Immun. **56:**1057–1060.
52. **Nowicki, B., J. Singhal, L. Fang, S. Nowicki, and C. Yallampalli.** 1999. Inverse relationship between severity of experimental pyelonephritis and nitric oxide production in C3H/HeJ mice. Infect. Immun. **67:**2421–2427.
53. **Nowicki, B., L. Truong, J. Moulds, and R. Hull.** 1988. Presence of the Dr receptor in normal tissues and its possible role in the pathogenesis of ascending urinary tract infection. Am. J. Pathol. **133:**1–4.
54. **Peiffer, I., A. L. Servin, and M.-F. Bernet-Camard.** 1998. Piracy of decay-accelerating factor (CD55) signal transduction by the diffusely adhering strain *Escherichia coli* C1845 promotes cytoskeletal F-actin rearrangements in cultured human intestinal INT407 cells. Infect. Immun. **66:**4036–4042.
55. **Peterson, M. D., and M. S. Mooseker.** 1992. Characterization of the enterocyte-like brush border cytoskeleton of the $C2_{BBe}$ clones of the human intestinal cell line, Caco-2. J. Cell Sci. **102:**581–600.
56. **Peterson, M. D., W. M. Bement, and M. S. Mooseker.** 1993. An *in vitro* model for the analysis of intestinal brush border assembly. II. Changes in expression and localization of brush border proteins during cell contact-induced brush border assembly in Caco-2_{BBe} cells. J. Cell Sci. **105:**461–472.
57. **Peterson, M. D., and M. S. Mooseker.** 1993. An *in vitro* model for the analysis of intestinal brush border assembly. I. Ultrastructural analysis of cell contact-induced brush border assembly in Caco-2_{BBe} cells. J. Cell Sci. **105:**445–460.
58. **Pham, T., A. Kaul, A., Hart, P. Goluszko, J. Moulds, S. Nowicki, D. M. Lublin, and B. J. Nowicki.** 1995. Dra-related X adhesins of gestational pyelonephritis-associated *Escherichia coli* recognize SCR-3 and SCR-4 domains of recombinant decay-accelerating factor. Infect. Immun. **63:**1663–1668.
59. **Pinto, M., S. Robine-Leon, M. D. Appay, M. Kedinger, N. Triadou, E. Dussaulx, B. Lacroix, P. Simon-Assmann, K. Haffen, J. Fogh, and A. Zweibaum.** 1983. Enterocyte-like differentiation and polarization of the human colon carcinoma cell line Caco-2 in culture. Biol. Cell **47:**323–330.
60. **Rhoads, J. M., R. C. Vogler, S. R. Lacey, R. L. Reddick, E. O. Keku, R. Azizkhan, and H. M. Berschneider.** 1991. Microvillus inclusion disease: in vitro jejunal electrolyte transport. Gastroenterology **100:**811–817.
61. **Salas, P. J., M. L. Rodriguez, A. L., Viciana, D. E. Vega-Salas, and H. P. Hauri.** 1997. The apical submembrane cytoskeleton participates in the organization of the apical pole in epithelial cells. J. Cell Biol. **21:**359–375.
62. **Schwartz, N., M. Hosford, R. M. Sandoval, M. C. Wagner, S. J. Atkinson, J. Bamburg, and B. A. Molitoris.** 1999. Ischemia activates actin depolymerizing factor: role in proximal tubule microvillar actin alterations. Am. J. Physiol. **276:**F544–F551.
63. **Sears, C. L., and J. B. Kaper.** 1996. Enteric bacterial toxins: mechanisms of action and linkage to intestinal secretion. Microbiol. Rev. **60:**167–215.
64. **Sogabe, K., N. F. Roeser, J. A. Davis, S. Nurko, M. A. Venkatachalam, and J. M. Weinberg.** 1996. Calcium dependence of integrity of the actin cytoskeleton of proximal tubule cell microvilli. Am. J. Physiol. **271:**F292–F303.
65. **Sun, H.-Q., K. Kwiatkowska, and H. L. Yin.** 1995. Actin monomer binding proteins. Curr. Opin. Cell Biol. **7:**102–110.
66. **Swanson, T. N., S. S. Bilge, B. Nowicki, and S. L. Moseley.** 1991. Molecular structure of the Dr adhesin: nucleotide sequence and mapping of receptor-binding domain by use of fusion constructs. Infect. Immun. **59:**261–268.
67. **Yamamoto, T., Y. Koyama, M. Matsumoto, E. Sonoda, S. Nakayama, M. Uchimura, W. Paveenkittiporn, K. Tamura, T. Yokoda, and P. Etcheverria.** 1992. Localized, affregative, and diffuse adherence to HeLa cells, plastic, and human small intestines by *Escherichia coli* isolated from patients with diarrhea. J. Infect. Dis. **166:**1295–1310.
68. **Zweibaum, A., M. Laburthe, E. Grasset, and D. Louvard.** 1991. Use of cultured cell lines in studies of intestinal cell differentiation and function, p. 223–255. *In* S. J. Schultz, M. Field, and R. A. Frizell (ed.), Handbook of physiology: the gastrointestinal system, vol. IV: intestinal absorption and secretion. American Physiological Society, Bethesda, Md.

Editor: V. J. DiRita